HHS Public Access

Author manuscript

Phytochemistry. Author manuscript; available in PMC 2016 May 27.

Published in final edited form as:

Phytochemistry. 2014 September ; 105: 79–84. doi:10.1016/j.phytochem.2014.06.011.

Asphodosides A-E, anti-MRSA metabolites from Asphodelus microcarpus

Mohammed M. Ghoneim[a,b], **Khaled M. Elokely**[d], **Atef A. El-Hela**[b], **Abd-Elsalam I. Mohammad**[b], **Melissa Jacob**[a], **Mohamed M. Radwan**[a,c], **Robert J. Doerksen**[a,d], **Stephen J. Cutler**[a,d], and **Samir A. Ross**[a,e,*]

[a] National Center for Natural Products Research, The University of Mississippi, University, MS 38677, USA

[b] Department of Pharmacognosy, Faculty of Pharmacy, The University of Al-Azhar, Cairo 11371, Egypt

[c] Department of Pharmacognosy, Faculty of Pharmacy, The University of Alexandria, Alexandria 21521, Egypt

[d] Department of Medicinal Chemistry, School of Pharmacy, The University of Mississippi, University, MS 38677, USA

[e] Department of Pharmacognosy, School of Pharmacy, The University of Mississippi, University, MS 38677, USA

Abstract

Bioassay guided fractionation of the ethanolic extract of *Asphodelus microcarpus* Salzm. et Viv. (Xanthorrhoeaceae or Asphodelaceae) resulted in isolation of five compounds identified as asphodosides A-E (**1**–**5**). Compounds **2**–**4** showed activity against methicillin resistant *Staphylococcus aureus* (MRSA) with IC_{50} values of 1.62, 7.0 and 9.0 μg/mL, respectively. They also exhibited activity against *Staphylococcus aureus* (non-MRSA) with IC_{50} values of 1.0, 3.4 and 2.2 μg/mL, respectively. The structure elucidation of isolated metabolites was carried out using spectroscopic data (1D and 2D NMR), optical rotation and both experimental and calculated electronic circular dichroism (ECD).

Keywords

Asphodelus microcarpus; Asphodelaceae; Electronic circular dichroism; MRSA

* Corresponding author at: National Center for Natural Products Research, The University of Mississippi, University, MS 38677, USA. Tel.: +1 662 915 1031; fax: +1 662 915 7989. ; Email: sross@olemiss.edu (S.A. Ross).

Appendix A. Supplementary data

Supplementary data associated with this article can be found, in the online version, at http://dx.doi.org/10.1016/j.phytochem.2014.06.011.

1. Introduction

The genus Asphodelus belongs to family Liliaceae which comprises 187 genera and 2500 species. It is a circum-Mediterranean genus, which includes five sections and is represented by 16 species (Lifante and Aguinagalde, 1996). *Asphodelus microcarpus* Salzm. et Viv. (Xanthorrhoeaceae or Asphodelaceae) is a stout robust herb with roots of several spindle-shaped tubers, widely distributed over the coastal Mediterranean region (Tackholm and Drar, 1954). Its bulbs and roots are used to treat ectodermal parasites, jaundice, psoriasis and microbial infections (Tackholm, 1974). Lipids, carbohydrates, sterols, triterpenes, anthraquinones and arylcoumarins have been isolated from *A. microcarpus* (El-Seedi, 2007). Anthraquinones and pre-anthraquinones are considered important chemotaxonomic markers for plants in the family Asphodelaceae (Van et al., 1995). Naphthalenes co-exist or couple with anthraquinones and pre-anthraquinones, thus indicating their biogenetic relationship (Yagi et al., 1978).

Anthraquinones are a class of natural compounds that consist of several hundred compounds that differ in the nature and positions of substituent groups (Schripsema et al., 1999). This class of compounds contains derivatives that consist of the basic structure of a 9, 10-anthraquinone moiety (Bajaj and Ishimaru, 1999). In continuation of efforts to search for new antimicrobial metabolites from *A. microcarpus* using biological activity guided fractionation, several anthraquinones showed activity against both methicillin resistant *Staphylococcus aureus* (MRSA) and *S. aureus* (Ghoneim et al., 2014, 2013), and five new compounds (1–5) were isolated and their antimicrobial activities were evaluated Fig. 1.

2. Results and discussions

Compound **1** (Asphodoside A) was obtained as an optically active yellowish amorphous powder. Its HREIMS gave an $[M–H]^-$ ion at *m/z* 639.1301 (calcd. for $C_{35}H_{27}O_{12}$, 639.1322), consistent with the molecular formula of $C_{35}H_{27}O_{12}$. The ^{13}C, DEPT, and HMQC NMR spectra of **1** (Table 1) displayed 35 carbon signals, including two methyl groups at δ21.7 (C-11) and 22.5 (C-11′) as well as three carbonyl carbons at δ194.5 (C-9), 183.0 (C-10) and 193.4 (C-9′); these data supported the interpretation that this compound is an anthraquinone-oxoanthrone derivative (Van et al., 1995). Its anthraquinone structure showed a singlet at δ7.39 (H-2), with the biogenetically expected methyl signal at δ21.7 (C-11). In addition, an ABX spin system was observed for three aromatic protons of the chrysophanol moiety which resonated at δ7.61 (1H, d, J = 8.0 Hz, H-5), 7.51 (1H, t, J = 8.0 Hz, H-6), and 7.30 (1H, d, J = 8.0 Hz, H-7), leaving C-4 at δ132.5 as the point of attachment to the oxoanthrone structure. The ^1H NMR spectroscopic pattern of the other half of the molecule showed a chrysophanol moiety, where the ABX pattern was replaced by a pair of deshielded *ortho*-coupled protons (Van et al., 1995) with an AX pattern at δ7.66 (1H, d, J = 8.0 Hz, H-3′) and δ8.12 (1H, d, J = 8.0 Hz, H-4′), respectively. This indicated that the point of attachment in this molecule is at C-2′ (δ129.6). In the ^1H NMR spectrum, the anomeric proton appeared at δ3.90 (1H, d, H-1″, J = 9.2 Hz) suggesting α β configuration (Yang et al., 2013). The upfield shift of the anomeric carbon resonancel at δ 86.3 (C-1″) in the ^{13}C NMR spectrum (Table 1) and the HMBC correlations from H-1″to C-10′ (Fig. 2) provided evidence that the sugar moiety was connected to the aglycone at

C-10′ to form an oxanthrone C-glycoside. Its HMBC spectrum exhibited cross-peaks from: H-2 to C-4 and C-1a; C-3 methyl protons to C-2, C-3 and C-4; H-5 to C-7, C-8a and C-10; H-6 to C-5a and C-8; H-7 to C-5 and C-8a; H-3′ to C-1′, C-4′a and C-4, confirming the point of attachment, from H-5′ to C-7′, C-8′a, C-10′ and from the C-6′ methyl protons to C-5′, C-6′ and C-7′, respectively (Fig. 2). To determine the identity of the C-sugar attached to C-10′, oxidative hydrolysis of **1** was carried out (Levy and Tang, 1995). From the aqueous layer of the hydrolysate, D-(+) xylose was identified based on its specific rotation value [$[\alpha]_D^{25}$ + 432 (*c* = 0.06, MeOH)] and retention time (2.76 min.) in GC after silylation using BSTFA compared to standard sugars. To determine the absolute configuration of the stereogenic center at C-10′, its ECD spectrum was measured and compared to calculated values for the R enantiomer. The experimental ECD spectrum showed a positive Cotton effect at 422 nm and a negative Cotton effect at 391 nm (Fig. 3). The CAM-B3LYP simulated ECD spectrum (Sang et al., 2012), generated from 40 excited states using Gaussian band shapes for the peaks, had peaks at 391 and 422 nm, similar to the experimental data. The calculated ECD of the R enantiomer showed excellent agreement with the experimental data. Therefore, structure **1** is asphodelin-10′-oxanthrone-(10′*R*)-β-D-xylopyranoside, (Asphodoside A).

Compound **2** (Asphodoside B) was obtained as a yellowish amorphous powder. Its HREIMS gave an $[M+H]^+$ ion at *m/z* 641.1799, consistent with the molecular formula of $C_{35}H_{28}O_{12}$. The ^1H and ^{13}C NMR spectroscopic data of compounds **1** and **2** were similar (Table 1), but gave opposite CD spectra suggesting a difference in configuration at C-10′. From the aqueous layer of the hydrolysate, D-(+) xylose was identified based on its specific rotation value [$[\alpha]_D^{25}$ + 440 (*c* = 0.04, MeOH)] and retention time (2.76 min.) in GC after silylation using BSTFA compared to standard sugars. The CD spectrum of **2** (Fig. 3) showed a Cotton effect opposite to that of **1**. Accordingly compound **2** was assigned as asphodelin-10′-oxanthrone-(10′*S*)-*β*-D-xylopyranoside (Asphodoside B).

Compound **3** (Asphodoside C) was obtained as a yellowish amorphous powder. The HREIMS gave an $[M+H]^+$ ion at *m/z* 641.1801, consistent with the molecular formula of $C_{35}H_{28}O_{12}$. The ^1H and ^{13}C NMR spectroscopic data of compounds **3** and **1** were similar. The experimental ECD spectrum showed a negative Cotton effect peak at 422 nm and a positive Cotton effect peak at 391 nm (Fig. 4) which is opposite to that of **1**. Also, oxidative hydrolysis of **3** was carried out. L-(+) arabinose was identified in the aqueous layer based on its specific rotation value [$[\alpha]_D^{25}$ + 97 (*c* = 0.05, MeOH)] and retention time (2.19 min.) in GC after silylation, compared to standard sugars. Accordingly, compound **3** was identified as asphodelin-10′-oxanthrone-(10′*S*)-*β*-L-arabinopyranoside (Asphodoside C).

Compound **4** (Asphodoside D) was obtained as a yellowish amorphous powder. Its HREIMS gave an $[M+H]^+$ ion at *m/z* 641.1777, consistent with the molecular formula of $C_{35}H_{28}O_{12}$. The ^1H and ^{13}C NMR spectroscopic data of compounds **3** and **4** were similar, but also showed opposite CD spectra, suggesting a difference in configuration at C-10′ as well (Table 1), Also, oxidative hydrolysis of **4** was carried out. L-(+) arabinose was identified based on its specific rotation value [$[\alpha]_D^{25}$ + 100 (*c* = 0.05, MeOH)] and retention time (2.19 min.) in

GC after silylation using BSTFA compared to standard sugars. The Cotton effects of **4** are opposite those of **3** (Fig. 4). Accordingly, compound **4** was identified as asphodelin-10′-oxanthrone-(10′*R*)-*β*-L-arabinopyranoside (Asphodoside D).

Compound **5** (Asphodoside E) was obtained as a yellowish amorphous powder. The HREIMS of **5** gave an $[M+H]^+$ ion at *m/z* 689.1860, consistent with the molecular formula of $C_{36}H_{32}O_{14}$. The ^{13}C NMR, DEPT, and HMQC of 5 (Table 1) displayed 36 carbon signals, including one methylene group at *δ* 63.0 (C-11) and one methyl group at 20.9 (C-11′), as well as two carbonyl carbons at *δ* 193.4 (C-9) and 192.8 (C-9′), supporting **5** to be a dimeric oxoanthrone derivative. One-half of the molecule displayed *meta*-coupled protons at *δ* 6.82 (1H, d, *J* = 2.5 Hz, H-2) and 6.88 (1H, d, *J* = 2.5 Hz, H-4), respectively. In addition, an ABX spin system was observed for three aromatic protons which resonated at *δ* 6.80 (1H, d, *J* = 8.0 Hz H-5), 7.39 (1H, t, *J* = 8.0 Hz, H-6), and 6.85 (1H, d, *J* = 8.0 Hz, H-7) of the chrysophanol moiety, leaving C-10 at *δ* 70.1 as the point of attachment to the other half of the molecule. The ^1H and ^{13}C NMR spectroscopic patterns of the other half of the molecule were similar to compound 1. The ^{13}C NMR spectroscopic data of the sugar moiety of **5** (Table 1) was also superimposed with those reported for D-(+) glucose (Ghoneim et al., 2013). Accordingly compound **5** was assigned as chrysalodin-10-oxanthrone-(10′*S*)-*β*-D-glucopyranoside (Asphodoside E).

Compounds **1**–**5** were evaluated for their antimicrobial activity. Compounds **2**–**4** showed activity against MRSA with IC_{50} values of 1.62, 7.0 and 9.0 μg/mL, respectively, and also exhibited activity against *S. aureus* with IC_{50} values of 1.0, 3.4 and 2.2 μg/mL, respectively.

3. Conclusion

Five new compounds (**1**–**5**) were isolated from A. microcarpus. The isolated secondary metabolites **2**–**4** showed activity against both methicillin resistant *S. aureus* (MRSA) and methicillin susceptible *S. aureus*.

4. Experimental

4.1. General experimental procedures

Optical rotations were determined with an Autopol IV instrument. IR spectra were obtained using a Bruker Tensor 27 instrument. CD spectra were measured on a JASCO J-715 spectrometer. The NMR spectra were recorded on a Bruker Avance DRX-500 instrument at 500 (^1H) and 125 MHz (^{13}C), and a Varian Mercury 400 MHz spectrometer at 400 (^1H) and 100 MHz (^{13}C). HRESIMS spectra were measured using a Bruker Bioapex-FTMS with electrospray ionization (ESI). Column chromatographic (CC) separations were performed on silica gel 60 (0.04–0.063 mm), whereas TLC employed precoated TLC plates with silica gel 60 F254 (0.2 mm, Merck). Semi-preparative HPLC (Waters Delta Prep 4000) was performed using Luna® RP-18 (5 μ, 250 mm, 10 mm). The mobile phases used for TLC analyses were: EtOAc:*n*-hexane(7:3), $CHCl_3$:-MeOH (9.5:0.5) and $CHCl_3$:MeOH (8:2). GC analyses were carried out on a ThermoQuest Trace 2000 GC, equipped with a single split/splitless capillary injector, a ThermoQuest AS2000 autosampler and a Phenomenex ZB-5 column (15 m × 0.25 mm × 0.25 lm, DB1), interfaced to a ThermoQuest-Finnigan and equipped with a Flame

Ionization Detector (FID). The injector temperature was 250 °C and 1 μL injections were performed in the splitless mode, with the splitless time set at 60 s, the split flow set at 50 mL/min and the septum purge valve set to close 60 s after injection. The oven temperature was raised from 70 to 270 °C (hold 20 min) at a rate of 5 °C/min, for a total run time of 60 min; the transfer line temperature was 250 °C. Hel was used as the carrier gas at a constant pressure of 20 psi.

4.2. Plant material

Tubers of *A. microcarpus* were collected from an area 70 km West of Marsa Matrouh, Egypt, during March 2011. The plant was authenticated by Dr. Ibrahim El-Garf, Professor of Plant Taxonomy, Cairo University, Egypt. A voucher specimen (AM 21) has been deposited in the Pharmacognosy Department, Faculty of Pharmacy, Al-Azhar University, Cairo, Egypt.

4.3. Antimicrobial assay

Compounds **1**–**5** were tested for antimicrobial activity against *S. aureus* ATCC 29213, methicillin-resistant *S. aureus* ATCC 33591 (MRSA), *Escherichia coli* ATCC 35218, *Pseudomonas aeruginosa* ATCC 27853, *Mycobacterium intracellulare* ATCC 23068, *Candida albicans* ATCC 90028, *Candida glabrata* ATCC 90030, *Candida krusei* ATCC 6258, *Cryptococcus neoformans* ATCC 90113, and *Aspergillus fumigatus* ATCC 204305, respectively, ciprofloxacin and amphotericin B were used as positive controls for bacteria and fungi, respectively (Bharate et al., 2007).

4.4. Oxidative hydrolysis

Compounds **1**–**4** (5 mg each) were separately treated 15 mL of 1 N ferric chloride/MeOH (1:1) at 100 °C, for four hours. The reaction mixture was evaporated, and the hydrolysate, after dilution with H_2O (20 mL), was extracted with EtOAc (3 × 20 mL). The EtOAc extracts were evaporated to afford the aglycones.

4.5. GC/FID trimethylsilyl derivatization

Dried aqueous layers of the hydrolysate of compounds **1**–**4** (ca. 100 μg each) were treated separately with pyridine (5 μL, silylation grade, Pierce) and BSTFA [N,O-bis(trimethylsilyl)trifluoroacetamide] (100 μL, 98+%, Acros Organics), followed by heating at 75 °C for 1 h. After cooling to room temperature, CH_2Cl_2 (0.9 mL) was added to the reaction mixture and the solution analyzed by GC/FID and compared with standard xylose and arabinose after derivatization.

4.6. Extraction and isolation

Air-dried powdered plant material (2 kg) was exhaustively extracted by maceration with EtOH (10 L × 3, 70:30, v/v/) at room temperature for 3 days. The combined extracts were evaporated under reduced pressure to afford a dry residue (400 g). The latter was subjected to vacuum liquid chromatography (VLC) on silica gel (1200 g) using 2.0 L each of petroleum ether, EtOAc and MeOH. Each fraction was evaporated to yield 20 g (Pet. ether), 210 g (EtOAc) and 15 g (MeOH) residuesw. The MeOH fraction (15 g) was subjected to vacuum liquid chromatography (VLC) on silica gel (600 g) using 1.0 L each of *n*-hexane, n-

hexane/EtOAc (50:50) and (25:75), EtOAc, EtOAc/MeOH (1:1) and MeOH to give six fractions (F1–F6). Fraction F5 (1.2 g) was applied to a silica gel column (100 g) to deliver eight subfractions (1–8). Subfraction 4 (100 mg) was subjected to subsequent purification on semi-preparative RP-C18 HPLC eluting with MeOH/H_2O (75:25) using Luna® RP-18 (5 μ, 250 mm, 10 mm) at a flow rate of 5.0 mL/min and detection at λ_{max} = 254 nm to give compounds **1** (30 mg, 48 min.), **2** (35 mg, 49 min.), **3** (20 mg, 45 min.) and **4** (30 mg, 46 min.), respectively. Subfraction 6 (50 mg) was subjected to subsequent purification on semipreparative RP-C_{18} HPLC eluting with MeOH/H_2O (60:40 v/v),using Luna® RP-18 (5 μ, 250 mm, 10 mm) at a flow rate of 5.0 mL/min and detection at 254 nm to give **5** (5 mg, 35 min.).

4.6.1. Asphodelin-10′-oxanthrone-(10′R)-β-D-xylopyranoside—*(Asphodoside A)*

(1): yellowish amorphous powder; $[\alpha]_D^{25}$ + 29.9 (*c* = 0.08, MeOH); IR (KBr) ν_{max} 2923, 2853, 1608, 1568,1451, 1422, 1279 cm^{-1}; UV (MeOH) λ_{max} (log ε): 210 (3.30), 220 (2.92), 240 (3.30), 250 (3.30), 380 (2.33) nm HRESIMS gave an $[M–H]^-$ ion at *m/z* 639.1301 (calcd. for $C_{35}H_{27}O_{12}$, 639.1322). For ^1H NMR and ^{13}C NMR spectroscopic data, see Table 1.

4.6.2. Asphodelin-10′-oxanthrone-(10′S)-β-D-xylopyranoside—*(Asphodoside B)*

(2): yellowish amorphous powder; $[\alpha]_D^{25}$ − 29.8 (*c* = 0.08, MeOH); IR (KBr) ν_{max} 3373, 1674, 1604, 1425, 1280 cm^{-1}; UV (MeOH) λ_{max} (log ε): 205 (2.86), 220 (2.90), 235 (3.30), 245 (3.30), 380 (2.30); HRESIMS gave an $[M+H]^+$ ion at *m/z* 641.1799 (calcd. for $C_{35}H_{29}O_{12}$, 641.1659). For ^1H NMR and ^{13}C NMR spectroscopic data, see Table 1.

4.6.3. Asphodelin-10′-oxanthrone-(10′S)-β-L-arabinopyranoside—*(Asphodoside C)* ***(3)***

: yellowish amorphous powder; $[\alpha]_D^{25}$ − 34.9 (*c* = 0.05, MeOH); IR (KBr) ν_{max} 2924, 2854, 1735, 1626, 1559, 1424, 1282, 1208 cm^{-1}; UV (MeOH) λ_{max} (log ε): 205 (3.39), 220 (2.98), 235 (3.03), 245 (3.39), 380 (2.41); HRESIMS gave an $[M+H]^+$ ion at *m/z* 641.1801 (calcd. for $C_{35}H_{29}O_{12}$, 641.1659). For ^1H NMR and ^{13}C NMR spectroscopic data, see Table 1.

4.6.4. Asphodelin-10′-oxanthrone-(10′R)-β-L-arabinopyranoside—*(Asphodoside D)* ***(4)***

: yellowish amorphous powder; $[\alpha]_D^{25}$ + 17.95 *c* = 0.05, MeOH); IR (KBr) ν_{max} 2923, 1558, 1425, 1281 cm^{-1}; UV (MeOH) λ_{max} (log ε): 210 (3.39), 220 (3.02), 235 (3.39), 245 (3.39), 375 (2.20); HRESIMS gave an $[M+H]^+$ ion at *m/z* 641.1777 (calcd. for $C_{35}H_{29}O_{12}$, 641.1659). For ^1H NMR and ^{13}C NMR spectroscopic data, see Table 1.

4.6.5. Chrysalodin-10-oxanthrone-(10′S)-β-D-glucopyranoside—*(Asphodoside E).*

(5): yellowish amorphous powder; $[\alpha]_D^{25}$ − 31.9 (*c* = 0.05, MeOH); IR (KBr) ν_{max} 2918, 1608, 1530, 1423, 1285 cm^{-1}; UV (MeOH) λ_{max} (log ε): 230 (3.39), 245 (3.39), 270 (2.43), 305 (2.45); HRESIMS gave an $[M+H]^+$ ion at *m/z* 689.1860 (calcd. for $C_{36}H_{33}O_{14}$, 689.1869). For ^1H NMR and ^{13}C NMR spectroscopic data, see Table 1.

Supplementary Material

Refer to Web version on PubMed Central for supplementary material.

Acknowledgements

We are grateful to the Egyptian Government and C06 RR14503 program from the NIH NCRR. The calculations were performed using the facilities of the Mississippi Center for Supercomputing Research (MCSR). This work is supported in part by United States Department of Agriculture ARS specific Cooperative Agreement No. 58-6408-2-0009.

References

Bajaj, Y.; Ishimaru, K. Transgenic Medicinal Plants. Vol. 22. Springer; 1999. Genetic Transformation of Medicinal Plants; p. 1-29.

Bharate SB, Khan SI, Yunus NA, Chauthe SK, Jacob MR, Tekwani BL, Khan IA, Singh IP. Antiprotozoal and antimicrobial activities of O-alkylated and formylated acylphloroglucinols. Bioorg. Med. Chem. 2007; 15:87–96. [PubMed: 17070063]

El-Seedi HR. Antimicrobial arylcoumarins from Asphodelus microcarpus. J. Nat. Prod. 2007; 70:118–120. [PubMed: 17253862]

Ghoneim MM, Ma G, El-Hela AA, Mohammad A, Kottob S, El-Ghaly S, Cutler SJ, Ross SA. Biologically active secondary metabolites from Asphodelus microcarpus. Nat. Prod. Commun. 2013; 8:1117–1119. [PubMed: 24079182]

Ghoneim MM, Elokely KM, Atef A, Mohammad AI, Jacob M, Cutler SJ, Doerksen RJ, Ross SA. Isolation and characterization of new secondary metabolites from Asphodelus microcarpus. Med. Chem. Res. 2014; 23:3510–3515.

Levy DDE, Tang PC. The Chemistry of C-glycosides. Access Online via Elsevier. 1995

Lifante ZD, Aguinagalde I. The use of random amplified polymorphic DNA (RAPD) markers for the study of taxonomical relationships among species of Asphodelus sect. Verinea (Asphodelaceae). Am. J. Bot. 1996; 83:949–953.

Sang YM, Yan LK, Wang JP, Su ZM. TDDFT studies on the electronic structures and chiroptical properties of mono-tin-substituted Wells-Dawson polyoxotungstates. J. Phys. Chem. A. 2012; 116:4152–4158. [PubMed: 22443144]

Schripsema J, Ramos-Valdivia A, Verpoorte R. Robustaquinones, novel anthraquinones from an elicited Cinchona robusta suspension culture. Phytochemistry. 1999; 51:55–60.

Tackholm, V. Students' Flora of Egypt. Illustrations, Coloured Illustrations. Cairo University; Beirut: 1974. p. 888

Tackholm V, Drar M. Flora of Egypt. Bull. Faculty Sci. Egypt. Univ. 1954:93–136.

Van WBE, Yenesew A, Dagne E. Chemotaxonomic significance of anthraquinones in the roots of Asphodeloideae (Asphodelaceae). Biochem. Syst. Ecol. 1995; 23:277–281.

Yagi A, Makino K, Nishioka I. Studies on the constituents of Aloe saponaria HAW. IV. The structures of bianthraquinoid pigments. Chem. Pharm. Bull. 1978; 26:1111–1116.

Yang Y, Yan YM, Wei W, Luo J, Zhang LS, Zhou XJ, Wang PC, Yang YX, Cheng YX. Anthraquinone derivatives from Rumex plants and endophytic Aspergillus fumigatus and their effects on diabetic nephropathy. Bioorg. Med. Chem. Lett. 2013; 23:3905–3909. [PubMed: 23683594]

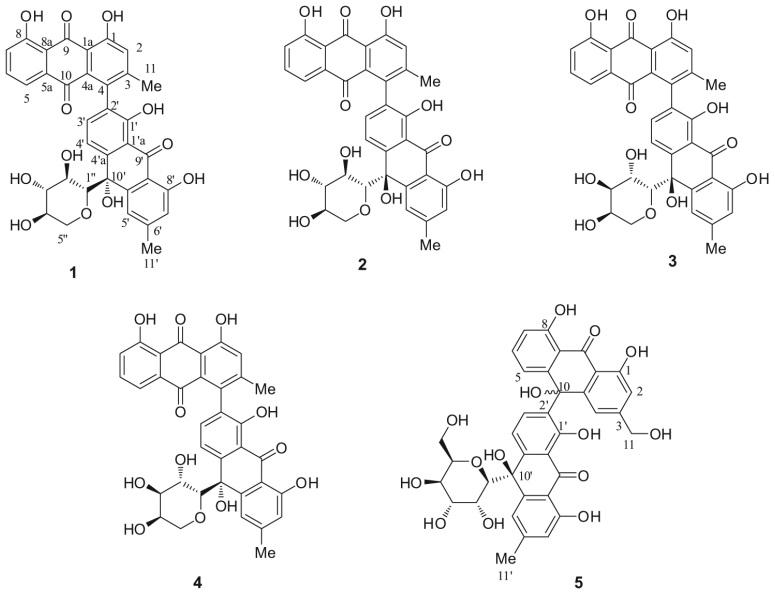

Fig. 1.
Chemical structures of Compounds 1–5.

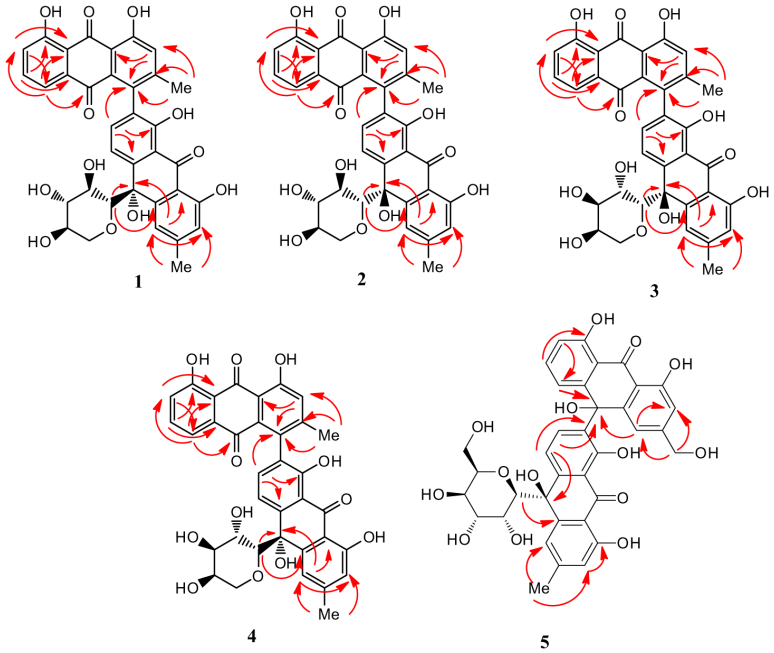

Fig. 2.
Key HMBC correlations of 1–5.

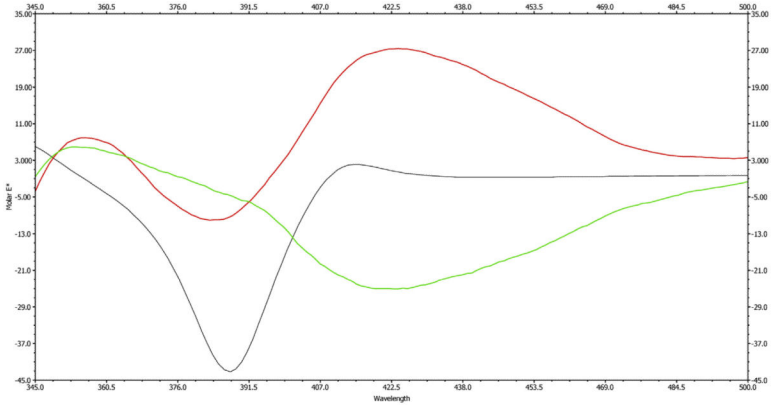

Fig. 3.

Experimental (red for 1 and green for 2) spectrum compared to the calculated (black) ECD spectrum of 1. The CAM-B3LYP calculated results were generated from 40 excited states. For the calculated ECD spectrum, the energy-weighted Boltzmann average for the two lowest-energy conformers is shown. The units of molar ellipticity are deg cm^2 dmol. (For interpretation of the references to colour in this figure legend, the reader is referred to the web version of this article.)

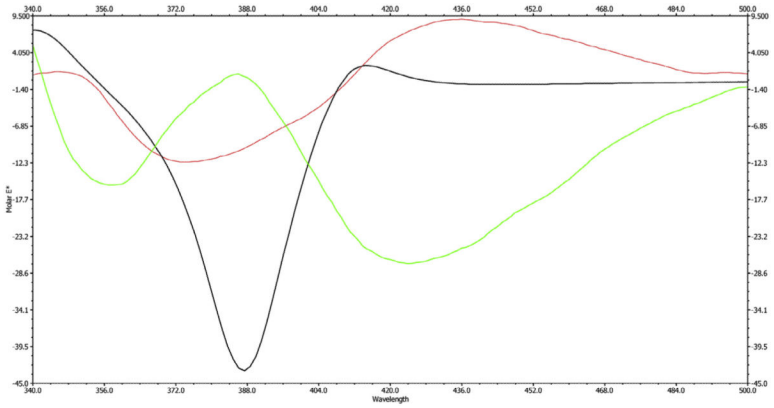

Fig. 4.

Experimental (red for 3 and green for 4) spectrum compared to the calculated (black) ECD spectrum of 1. The CAM-B3LYP calculated results were generated from 40 excited states. For the calculated ECD spectrum, the energy-weighted Boltzmann average for the two lowest-energy conformers is shown. The units of molar ellipticity are deg cm^2 dmol. (For interpretation of the references to colour in this figure legend, the reader is referred to the web version of this article.)

Table 1

^{1}H and ^{13}C-NMR spectroscopic data (400 MHz) for compounds **1, 2** and **4** in pyridin-d_5 and ^{1}H and ^{13}C-NMR spectroscopic data for compounds **3** (400 MHz) and 5 (500 MHz) in CD_3OD-d_4[a].

Position	1		2		3		4		5	
	δ_C	δ_H (*J* in Hz)	δ_C	δ_H (*J* in Hz)	δ_C	δ_H (*J* in Hz)	δ_C	δ_H (*J* in Hz)	δ_C	δ_H (*J* in Hz)
1	163.2	–	162.9	–	163.6	–	162.4	–	162.1	–
2	126.0	7.39 (s)	125.5	7.30 (s)	126.0	7.20 (s)	125.8	7.30 (s)	113.3	6.82 (d, 2.5)
3	151.0	–	150.6	–	151.4	–	151.0	–	151.6	–
4	132.5	–	132.0	–	132.7	–	132.5	–	116.8	6.88 (d, 2.5)
5	137.1	7.61 (d, 8.0)	136.2	7.60 (d, 8.0)	136.0	7.22 (d, 8.0)	135.6	7.41 (d, 8.0)	118.9	6.80 (d, 8.0)
6	137.9	7.51 (t, 8.0)	137.4	7.55 (t, 8.0)	138.4	7.42 (t, 8.0)	137.7	7.39 (t, 8.0)	136.1	7.39 (t, 8.0)
7	124.4	7.30 (d 8.0)	123.9	7.27 (d 8.0)	124.7	7.00 (d)	124.2	7.25 (d 8.0)	116.0	6.85 (d 8.0)
8	162.6	–	162.3	–	162.7	–	162.6	–	161.8	–
9	194.5	–	194.1	–	194.1	–	194.5	–	193.4	–
10	183.0	–	182.3	–	183.6	–	182.5	–	70.1	–
1a	115.8	–	115.3	–	115.9	–	115.7	–	115.7	–
4a	132.1	–	131.6	–	132.5	–	132.0	–	148.9	–
5a	135.4	–	134.8	–	130.4	–	135.2	–	148.4	–
8a	116.5	–	116.1	–	115.3	–	116.4	–	114.4	–
1′	159.4	–	159.0	–	160.1	–	160.2	–	157.3	–
2′	129.6	–	129.2	–	135.4	–	129.8	–	134.1	–
3′	120.1	7.66 (d, 8.0)	119.7	7.50 (d, 8.0)	120.7	7.24 (d, 8.0)	120.2	7.48 (d, 8.0)	131.8	8.50 (d, 8.0)
4′	118.3	8.12 (d, 8.0)	118.0	8.10 (d, 8.0)	119.2	7.42 (d, 8.0)	119.5	8.10 (d, 8.0)	115.7	7.6 (d, 8.0)
5′	120.4	7.77 (d, 1.6)	120.0	7.70 (d, 1.6)	118.9	7.30 (d, 1.6)	119.1	7.88 (d, 1.6)	118.8	7.24 (d, 2.5)
6′	147.9	–	147.6	–	149.5	–	149.0	–	147.1	–
7′	118.1	6.86 (d, 1.6)	117.8	6.80 (d, 1.6)	118.1	6.67 (d, 1.6)	118.0	6.90 (d, 1.6)	116.7	6.71 (d, 2.5)
8″	163.2	–	162.7	–	162.8	–	163.2	–	161.7	–
9′	193.4		192.8		194.6		193.4		192.8	
10′	77.1		76.8		77.1		77.5		75.0	
1′a	117.4		116.8		117.6		117.4		115.7	
4′a	149.1		148.7		144.9		146.2		146.6	

Position	1		2		3		4		5	
	δ_C	δ_H (*J* in Hz)	δ_C	δ_H (*J* in Hz)	δ_C	δ_H (*J* in Hz)	δ_C	δ_H (*J* in Hz)	δ_C	δ_H (*J* in Hz)
5′a	147.2		146.9		149.5		150.1		145.0	
8′a	115.5		116.8		116.5		115.6		113.8	
1″	86.3	3.90 (d, 9.2)	85.6	3.90 (d, 8.4)	86.1	3.26 (d, 8.4)	86.0	3.90 (d, 8.4)	84.3	3.30 (d, 8.4)
2″	73.5	3.26 (m)	73.1	4.09 (m)	73.0	3.26 (m)	73.6	3.26 (m)	78.3	3.28 (m)
3″	80.6	3.28 (m)	80.1	4.13 (m)	79.8	3.28 (m)	80.5	3.28 (m)	80.6	2.97 (m)
4″	72.0	2.86 (1H, m)	71.6	3.50 (1H, m)	73.0	2.86 (1H, m)	72.0	2.86 (1H, m)	71.6	2.90 (1H, m)
5″	70.9	2.83 (m)	70.60	3.80 (m)	71.0	2.83 (m)	71.1	2.83 (m)	70.3	2.80 (m)
6″	–	–	–	–	–	–	–	–	61.8	3.50, 3.26 (m))
11	21.7	2.22 (s)	21.5	2.16 (s)	21.6	2.08 (s)	21.9	2.10 (s)	63.0	4.52 (s)
11′	22.5	2.11 (s)	22.1	2.13 (s)	22.6	2.39 (s)	22.8	2.3 (s)	20.9	2.40 (s)

[a]Assignment was confirmed by DEPT135, HMQC, ^{1}H NMR and ^{13}C NMR experiments.